

ISOTOPIC COMPOSITION OF SOLAR ENERGETIC PARTICLE EVENTS MEASURED BY *ADVANCED COMPOSITION EXPLORER/ULEIS*

J. R. DWYER

Department of Physics and Space Sciences, Florida Institute of Technology, Melbourne, FL 32901; dwyer@pss.fit.edu

G. M. MASON¹

Department of Physics, University of Maryland, College Park, MD 20742; Glenn.Mason@umail.umd.edu

J. E. MAZUR

Aerospace Corporation, El Segundo, CA 90245; joseph.mazur@aero.org

R. E. GOLD AND S. M. KRIMIGIS

Johns Hopkins University, Applied Physics Laboratory, Laurel, MD 20723; robert.gold@jhuapl.edu, krimism1@spacemsg.jhuapl.edu

AND

E. MÖBIUS AND M. POPECKI

University of New Hampshire, Durham, NH 03824; eberhard.moebius@unh.edu, mark.popecki@unh.edu

Received 2001 May 22; accepted 2001 August 7

ABSTRACT

Since its 1997 August launch, the Ultra Low Energy Isotope Spectrometer (ULEIS) on board the *Advanced Composition Explorer (ACE)* has observed a large number of solar energetic particle (SEP) events in the 0.4–3 MeV nucleon⁻¹ range. These events show remarkable variability of both the elemental and isotopic compositions, with ²²Ne/²⁰Ne varying, from event to event, by up to a factor of 10, Fe/O by up to a factor of 100, and ³He/⁴He by up to a factor of 10⁴. In this paper we present new measurements of the ²²Ne/²⁰Ne, ²⁶Mg/²⁴Mg, and ³He/⁴He ratios at ~1 MeV nucleon⁻¹ and compare these ratios to the iron abundances measured during the same time periods. We find that the elemental abundances, Fe/O and Fe/Mg, and the isotopic abundances, ²²Ne/²⁰Ne and ²⁶Mg/²⁴Mg, are all well ordered by both the ³He/⁴He ratio and the average Fe charge state as measured by *ACE/SEPICA*. These variations in ²²Ne/²⁰Ne and ²⁶Mg/²⁴Mg are much larger than expected from the charge to mass dependence derived for the elemental abundances, and we suggest that the large fluctuations seen for the neon and magnesium isotopes are related to the amount of impulsive flare material present.

Subject headings: acceleration of particles — cosmic rays — interplanetary medium — solar wind — Sun: flares — Sun: particle emission

1. INTRODUCTION

The composition of solar energetic particles (SEPs) varies greatly from event to event, with ratios such as Fe/O varying over 2 orders of magnitude. In recent years, it has become clear that part of this variation is due to the fact that there are two kinds of SEP events, each with its own average composition: the large “gradual” events are believed to be accelerated at shock waves, driven from the Sun by coronal mass ejections (CMEs), and the smaller “impulsive” events are believed to be accelerated in solar flares closer to the Sun (e.g., Gosling 1993; Reames 1999; Lee 2000). The gradual events have, on average, abundances closer to the corona and the solar wind, and the impulsive events usually have large enhancements in the heavy elements and often have enormous enhancements in the ³He/⁴He ratio. With the launch of the *Advanced Composition Explorer (ACE)* in 1997 August, it has become clear that the classification of SEP events into gradual and impulsive categories is not so clear when based upon the particle measurements at 1 AU, with many large, apparently gradual events associated with CMEs having impulsive-like compositions, including ³He enhancements (Mason et al. 1999a). These observations have renewed interest in how abundance variations arise in SEP events and whether there is a relationship between the energetic

particles measured in impulsive events and those measured in gradual events.

Since it is difficult to imagine how the mass alone could affect the injection and subsequent acceleration of energetic particles, the fractionation of SEP abundances is usually assumed to be governed by the ratio of the ion’s charge to mass, Q/A . Indeed, if the energetic particles can be regarded as test particles in an electromagnetic field, then, as a result of the nature of the Lorentz force, their behavior should be completely determined by their velocity and Q/A . For a constant kinetic energy per nucleon, we therefore expect Q/A to be the only parameter that enters into the acceleration of the heavy ions. Because SEPs with $Z > 8$ are not usually stripped of all their electrons, different SEP species can have different Q/A values. Consequently, by measuring the composition of SEPs, we can gain insight into the injection and acceleration mechanisms involved in producing these particles.

Breneman & Stone (1985) found that in large SEP events, for nuclei heavier than helium, the deviations from the average abundances often followed a power law in Q/A . For impulsive events, associated with flares, the average abundances also show a trend in Q/A , with smaller Q/A values having larger enhancements, but they do not typically follow a power law. Furthermore, for some SEP events, the ³He/⁴He ratio is observed to be enhanced by as much as a factor of 10⁴ compared with the solar wind values of 4.8×10^{-4} (Ogilvie et al. 1980; Hsieh & Simpson 1970;

¹ Also Institute for Physical Science and Technology.

Reames, von Rosenvinge, & Lin 1985; Reames, Meyer, & von Rosenvinge 1994; Mason, Dwyer, & Mazur 2000). The enhancement of ^3He does not follow the same pattern as the heavier elements, since the Q/A for ^3He and ^4He would predict a ^3He depletion, rather than an enhancement. Indeed, the unique value of $Q/A = \frac{2}{3}$ for ^3He provides evidence that for ^3He -rich ($^3\text{He}/^4\text{He} > 0.01$) events, wave particle interactions play an important role in accelerating particles (Fisk 1978; Temerin & Roth 1992).

With the launch of the *ACE* spacecraft in 1997, it has become possible to measure the isotopic and elemental composition in SEP events for a broad range of event intensities and energies, allowing us to address the question of whether or not the isotopes show a Q/A fractionation similar to the elements. Compared to the solar photosphere, the elemental abundances of energetic particles are slightly complicated by their dependence upon the first ionization potential (FIP), with high-FIP elements appearing underabundant compared to the low-FIP elements (Meyer 1985). This effect, which is also observed in the solar wind and in galactic cosmic rays, cannot arise during acceleration, since the elements are stripped of their outer-shell electrons by the time acceleration begins. Therefore, in order to study the acceleration mechanisms, we wish to eliminate the effects due to the FIP. The isotopic abundances have the advantage that all the isotopes of a given element have the same FIP. In addition, when comparing variations in the neon and magnesium isotopic abundances with the iron abundances, we use the Fe/Mg ratio instead of the more traditional Fe/O ratio, since, unlike Fe and O, Fe and Mg have very similar FIPs (7.65 and 7.87 eV, respectively).

In addition to having the same FIP, the charge states of the isotopes should be the same for a given element, allowing the Q/A dependencies to be easily studied. Results from the *ACE/SIS* instrument in the 24–72 MeV nucleon $^{-1}$ range show that the variations in the heavier isotopic abundances are well correlated with variations in the Fe/O abundance (Leske et al. 1999). However, whether or not the magnitude of the fluctuations for the isotopes is consistent with those seen for Fe/O has not been thoroughly tested, since the charge states are not known for most of the events in the SIS energy range. Furthermore, because the charge states for SEPs are known to be energy dependent, the charge states measured at lower energies may not apply above 10 MeV nucleon $^{-1}$ (Mazur et al. 1999). In contrast, *ACE/ULEIS*, which measures particles at energies near 1 MeV nucleon $^{-1}$, is closer to the 0.18–0.75 MeV nucleon $^{-1}$ energy range of *ACE/SEPICA* (Möbius et al. 1998), which provides charge state measurements for many of the same events.

2. OBSERVATIONS

The Ultra Low Energy Isotope Spectrometer (ULEIS) is part of *ACE*, launched in 1997 August (Mason et al. 1998). The *ACE* spacecraft contains a large collection of modern instruments designed to measure elemental and isotopic composition over an energy range covering the solar wind up through galactic cosmic rays. The ULEIS instrument is a time of flight mass spectrometer with a geometry factor of 1 cm 2 sr, designed to measure protons through gold in the energy range ~ 0.02 –10 MeV nucleon $^{-1}$. The excellent mass resolution ($\sigma < 0.2$ amu for oxygen at 1 MeV nucleon $^{-1}$) and low background of ULEIS allow precise isotopic measurements of SEPs that were unavailable

before *ACE*. In particular, ULEIS measures $^3\text{He}/^4\text{He}$ to values as low as 0.001, allowing correlations with the ^3He abundance to be studied over a much broader range than was previously possible.

In addition, the Solar Energetic Particle Ionic Charge Analyzer (SEPICA), also on board the *ACE* spacecraft, uses gas-filled proportional counters and solid state detectors to measure the charge states of energetic ions in the 0.2–5 MeV nucleon $^{-1}$ range (Möbius et al. 1998). The charge state information provides valuable information about sources of the energetic particles, i.e., whether they originate at hot flare sites or in the cooler corona or solar wind.

We have analyzed ULEIS data for the period 1997 October 31–2000 January 29 and have selected 67 events for this study, based upon the 0.4–3.0 MeV nucleon $^{-1}$ Mg and Fe intensities. Of these events, 45 had adequate statistics to measure both $^{22}\text{Ne}/^{20}\text{Ne}$ and $^3\text{He}/^4\text{He}$. Since the focus of this study is SEP events, we have excluded periods that were clearly associated with local interplanetary shocks or corotating interaction regions.

Figure 1 shows the ULEIS mass histograms in the 1.0–2.0 MeV nucleon $^{-1}$ energy range for all the time periods with $^3\text{He}/^4\text{He} < 0.01$ (top panel) and all the time periods with $^3\text{He}/^4\text{He} > 0.1$ (bottom panel). Note the large enhancements in the $^{22}\text{Ne}/^{20}\text{Ne}$ and $^{26}\text{Mg}/^{24}\text{Mg}$ ratios in the ^3He -“high” ($^3\text{He}/^4\text{He} > 0.1$) data compared with the ^3He -“low” ($^3\text{He}/^4\text{He} < 0.01$) data, despite only modest changes in the elemental abundances. Similar enhancements were seen by Mason, Mazur, & Hamilton (1994) in ^3He -rich flares. The average abundances for these two data sets shown in Figure

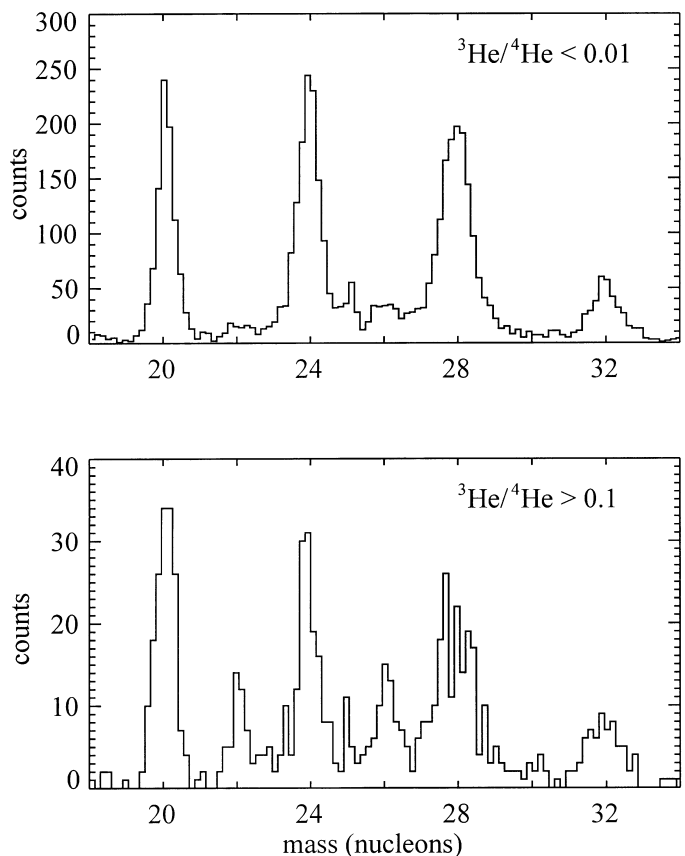


FIG. 1.—Mass histogram for all time periods with $^3\text{He}/^4\text{He} < 0.01$ (top panel) and $^3\text{He}/^4\text{He} > 0.1$ (bottom panel).

TABLE 1
AVERAGE ABUNDANCE RATIOS AND FLUENCES OF ³He-“Low” AND ³He-“High” DATA

Measured Quantities	³ He-“Low” (³ He/ ⁴ He < 0.1)	³ He-“High” (³ He/ ⁴ He > 0.1)	Solar Wind	Solar Wind References
³ He/ ⁴ He	0.0023 ± 0.0002	0.296 ± 0.002	4.8 × 10 ⁻⁴	1
Fe/Mg	1.08 ± 0.01	3.11 ± 0.05	0.796	2
²² Ne/ ²⁰ Ne	0.10 ± 0.01	0.31 ± 0.05	0.073	3
²⁶ Mg/ ²⁴ Mg	0.18 ± 0.02	0.51 ± 0.07	0.146	4
Combined oxygen fluences ^a (cm ² sr MeV) ⁻¹	4.0 × 10 ⁵	1.1 × 10 ⁴
Total time accumulated (s)	8.1 × 10 ⁶	5.8 × 10 ⁶

^a 0.4–3.0 MeV nucleon⁻¹.

REFERENCES.—(1) Ogilvie et al. 1980. (2) von Steiger et al. 2000. (3) Anders & Ebihara 1982. (4) Wimmer-Schweingruber et al. 1999.

1 are listed in Table 1 along with the solar wind values, combined fluences, and total accumulation times.

As can be seen in Table 1, the average values of Fe/Mg, ²²Ne/²⁰Ne, and ²⁶Mg/²⁴Mg are all much larger in the ³He-“high” data set. This trend can also be seen in the abundances calculated for individual events. Figure 2 shows the ²²Ne/²⁰Ne versus Fe/Mg and ³He/⁴He abundances for the individual SEP events of this study. ²²Ne/²⁰Ne is measured at 0.8–3.0 MeV nucleon⁻¹, Fe/Mg at 0.4–3.0 MeV nucleon⁻¹, and ³He/⁴He at 0.5–1.5 MeV nucleon⁻¹, ranges that give the optimum mass resolution and counting statistics for the measurements. Instead of plotting error bars, which visually tend to overemphasize the data with lower

statistical precision, we represent the statistical errors in the plot with circles, the area of each circle being proportional to one over the relative error of the data point. While there is considerable scatter in the data, the ²²Ne/²⁰Ne ratio shows positive correlations with both Fe/Mg and ³He/⁴He. If the abundances are determined by a monotonic dependence on *Q/A*, then a correlation between ²²Ne/²⁰Ne and Fe/Mg is not surprising, although the large magnitude of the enhancements in the ²²Ne/²⁰Ne ratio is not so easy to account for. However, a monotonic dependence on *Q/A* cannot explain the correlation between ²²Ne/²⁰Ne and ³He/⁴He since an anticorrelation would be expected in this case. The correlation seen in both panels in Figure 2 could arise from the fact that the iron abundance is also correlated with the ³He abundance. This is most easily seen by plotting Fe/O (which has a higher statistical accuracy than Fe/Mg) versus ³He/⁴He.

The dependence of the elemental abundance Fe/O on the ³He/⁴He ratio is plotted in Figure 3, which shows the average abundances for the events of this study. The Fe/O ratio is measured in the 0.4–3.0 MeV nucleon⁻¹ energy range, and ³He/⁴He is measured in the 0.5–1.5 MeV nucleon⁻¹ range. Figure 4 is similar to Figure 3 except that

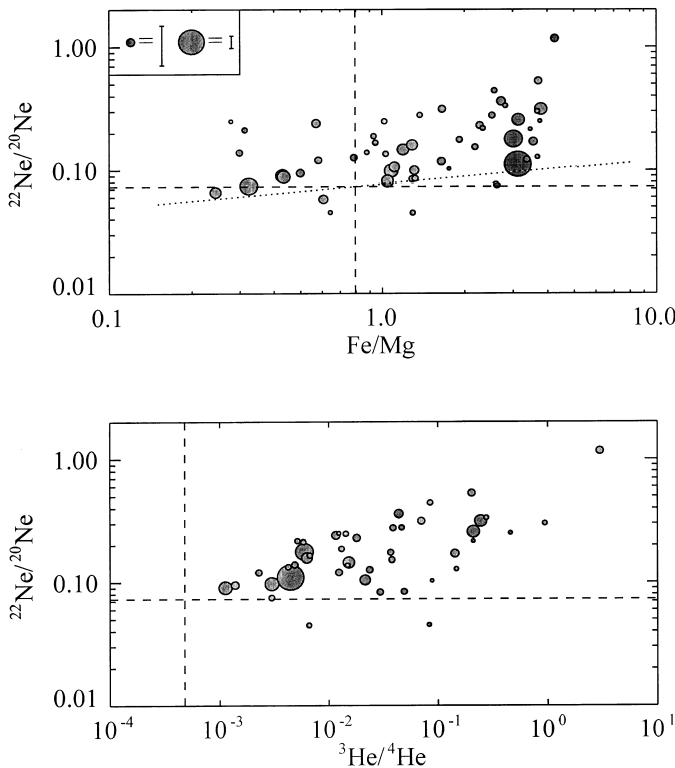


FIG. 2.—²²Ne/²⁰Ne vs. Fe/Mg (top panel) and ³He/⁴He (bottom panel) for the individual SEP events of this study. The dashed lines show the solar wind values for the abundances (von Steiger et al. 2000; Ogilvie et al. 1980). The dotted line shown in the top panel is the result of the Breneman & Stone (1985) model, assuming that *Q_{Mg}/Q_{Fe}* = 0.7 for all the events. The area of each circle is proportional to one over the relative error. The inset in the top panel shows the relationship between the circle size and error bars for the relative errors 0.35 and 0.11.

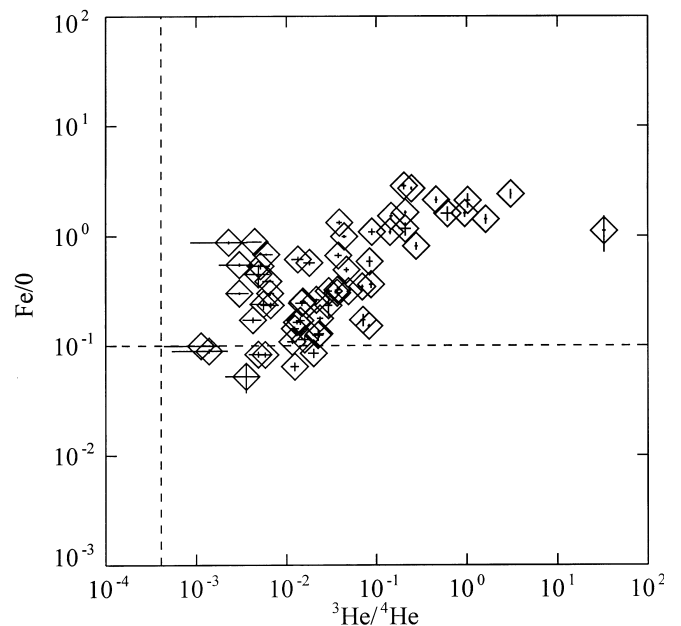


FIG. 3.—Event-averaged Fe/O vs. ³He/⁴He. The dashed lines correspond to the solar wind values.

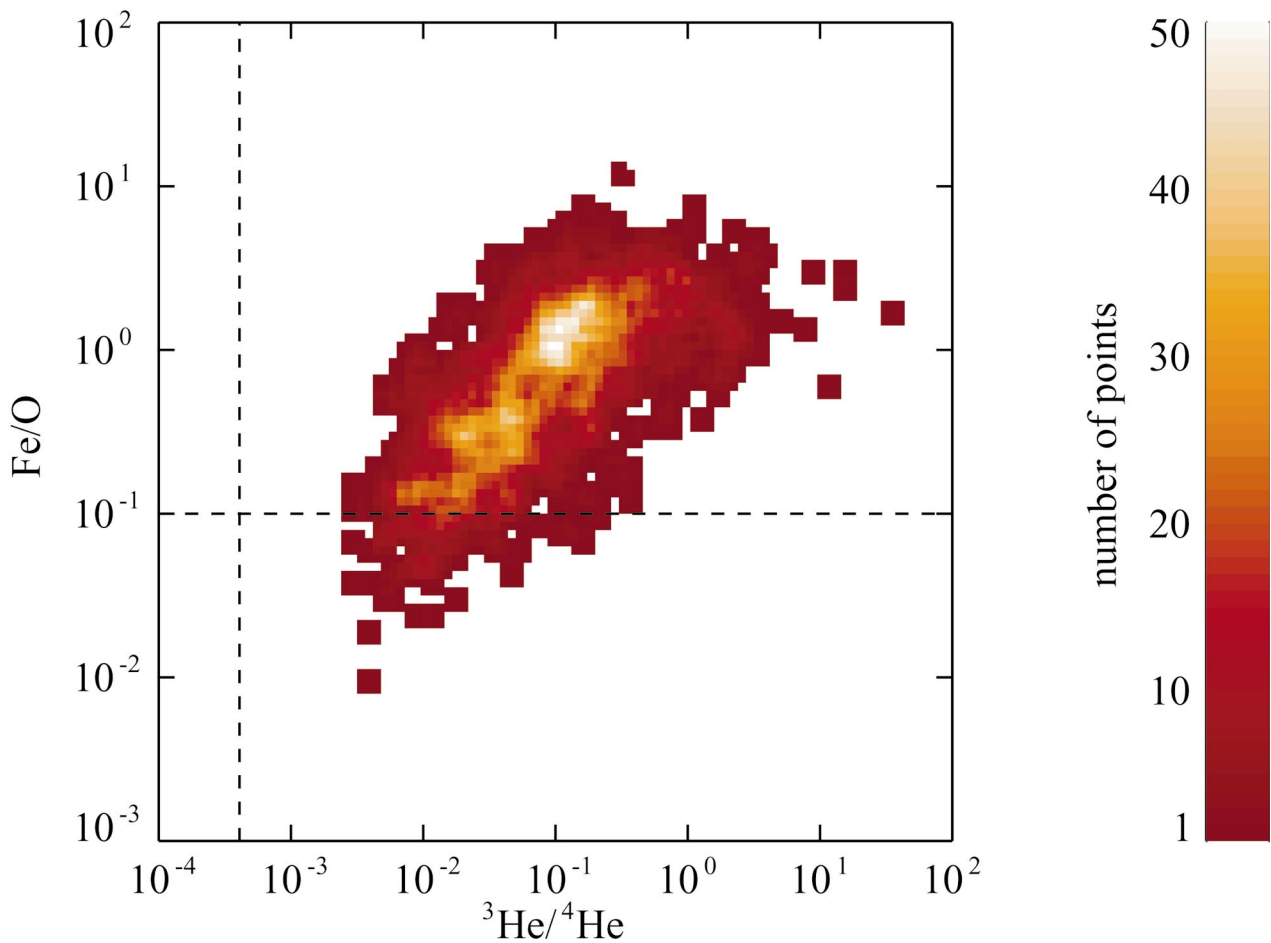


FIG. 4.—Fe/O vs. ${}^3\text{He}/{}^4\text{He}$. Unlike Fig. 3, which shows event averages, the data points here are mostly 1 hr averages. The color scale indicates the number of data points (*squares*) overlapping at any given location on the plot, and the dashed lines correspond to the solar wind values.

instead of event averages, each data point represents the average abundance measured over a time period extending from 1 up to 24 hr, depending upon the intensity of the period, with no attempt made to separate individual events. The accumulation interval is chosen so that at least five iron, five oxygen, and five ${}^4\text{He}$ counts are observed. The values of ${}^3\text{He}/{}^4\text{He}$ in Figures 3 and 4 extend to much lower values than previously observable, and a clear correlation between Fe/O and ${}^3\text{He}/{}^4\text{He}$ can be seen in the data. (The cutoff of the data at ${}^3\text{He}/{}^4\text{He} \sim 0.001$ is an instrumental effect.) Note that the good correlation seen over the entire ${}^3\text{He}/{}^4\text{He}$ range appears substantially weaker when limiting the data to ${}^3\text{He}/{}^4\text{He} > 0.1$, the range used by Mason et al. (1986) and Reames et al. (1994) when they reported seeing no correlation between Fe/O and ${}^3\text{He}/{}^4\text{He}$.

Presumably, the low ${}^3\text{He}/{}^4\text{He}$ data correspond to gradual, CME-associated events, and the high ${}^3\text{He}/{}^4\text{He}$ data correspond to impulsive, flare-associated events. However, the fact that the two classes of data merge together so smoothly is somewhat surprising and suggests that mixing of the two classes of events may occur. This smooth transition between ${}^3\text{He}$ -“low” and ${}^3\text{He}$ -“high” data is made more clear in Figure 5, which shows the average Fe/O abundances relative to the solar wind when the data in Figure 4 are binned according to the ${}^3\text{He}/{}^4\text{He}$ values. The error bars in Figure 5 show the rms fluctuations of the data in Figure 4 and not the standard error of the mean, which is much smaller than the errors shown.

The dependence of ${}^{22}\text{Ne}/{}^{20}\text{Ne}$, ${}^{26}\text{Mg}/{}^{24}\text{Mg}$, and Fe/Mg on the ${}^3\text{He}/{}^4\text{He}$ ratio is shown in Figure 6. Each data point in the figure is calculated from the sum of all 1 hr time periods with ${}^3\text{He}/{}^4\text{He}$ within the specified range. ${}^3\text{He}/{}^4\text{He}$ is

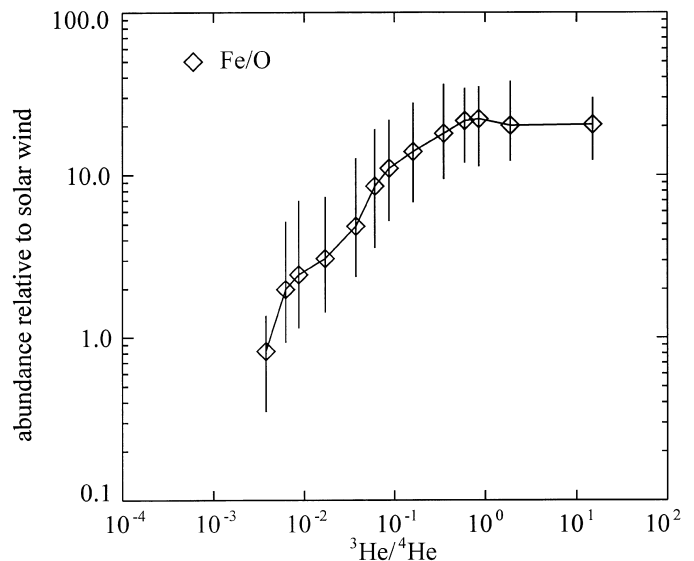


FIG. 5.—Average Fe/O ratio with respect to the solar wind value (0.10) as a function of the ${}^3\text{He}/{}^4\text{He}$ ratio. The error bars represent the rms scatter of the data points in Fig. 4 about the mean.

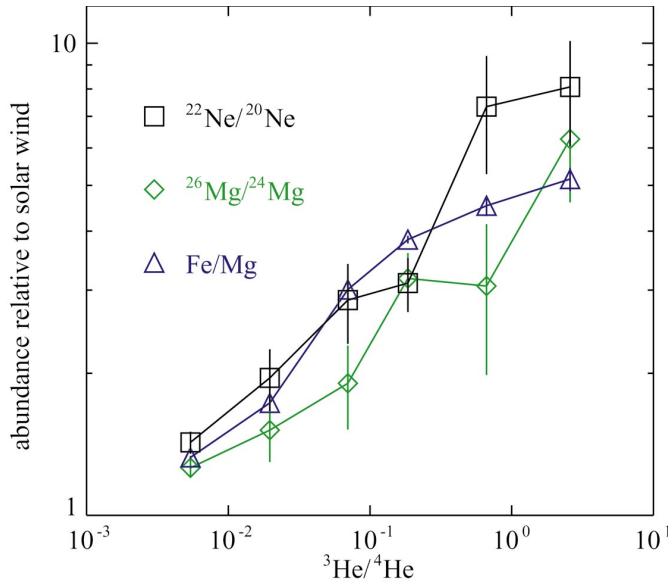


FIG. 6.— $^{22}\text{Ne}/^{20}\text{Ne}$, $^{26}\text{Mg}/^{24}\text{Mg}$, and Fe/Mg abundances with respect to the solar wind values vs. $^3\text{He}/^4\text{He}$.

measured at 0.5–1.5 MeV nucleon⁻¹, and the others are measured at 0.8–3.0 MeV nucleon⁻¹. Like the Fe/O data, the isotopes and Fe/Mg show a smooth and significant increase as a function of $^3\text{He}/^4\text{He}$. Impulsive flare material is known to be substantially hotter (i.e., have higher charge states) than CME-associated material. It is therefore not unexpected that the data also show a similar trend when plotted against the average iron charge states. Figure 7 shows the ACE/ULEIS $^{22}\text{Ne}/^{20}\text{Ne}$, $^{26}\text{Mg}/^{24}\text{Mg}$, and Fe/Mg abundances with respect to the solar wind values versus the average iron charge state as measured by ACE/

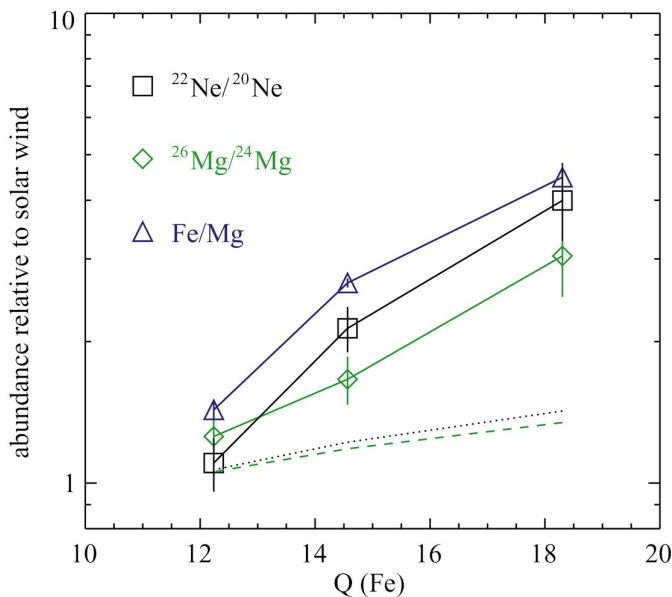


FIG. 7.— $^{22}\text{Ne}/^{20}\text{Ne}$, $^{26}\text{Mg}/^{24}\text{Mg}$, and Fe/Mg abundances with respect to the solar wind values vs. the average iron charge state as measured by ACE/SEPICA. The data points are the average of 20 SEP events that were binned together according to the measured Fe charge. The dotted black line shows the $^{22}\text{Ne}/^{20}\text{Ne}$, and the dashed green line shows the $^{26}\text{Mg}/^{24}\text{Mg}$ values predicted by the Breneman & Stone (1985) (power law in Q/A) relationship using the measured charge states and abundances of Fe/Mg.

SEPICA. The data points, which include 20 SEP events measured simultaneously by ULEIS and SEPICA, are binned according to the measured Fe charge of the events, after which the abundances were calculated. Möbius et al. (2000) reported similar correlations in the Ne/O and Fe/O ratios with the Fe charge states.

3. DISCUSSION

Breneman & Stone (1985) found that the enhancements and depletions of the elemental abundances of SEP events with respect to the value averaged over many events could be fitted with a power law in the charge-to-mass ratio, Q/A . Because the technique measures deviations from the mean, this power-law index necessarily has both positive and negative values. We note that a relationship of this form is not surprising, since plotted on a log scale, a power-law fit simply represents the first two terms in a Taylor expansion in $\log(Q/A)$. Because Q/A has a very small range of values, typically 0.5–0.25, it is reasonable that the first two terms are sufficient to approximate whatever complicated Q/A dependence may exist. This is especially true given that more complicated dependencies tend to be smoothed out when comparing the individual abundances to averages over many events. Furthermore, the small range in Q/A also means that, on a log scale, the difference between an expansion in $\log(Q/A)$ (power law) or Q/A (exponential) is not significant.

If the Breneman & Stone (1985) relationship is correct for the $^{22}\text{Ne}/^{20}\text{Ne}$ and Fe/Mg abundances, assuming $Q_{\text{Mg}}/Q_{\text{Fe}} = 0.7$ (which remains approximately true even as Q_{Fe} and Q_{Mg} vary over a broad range of temperatures), then $^{22}\text{Ne}/^{20}\text{Ne}$ should change as a power law in Fe/Mg with a power-law index of 0.2 (dotted line, Fig. 2, top panel). If both the elemental and isotopic abundances were completely described by a power law in Q/A , then we would expect that the $^{22}\text{Ne}/^{20}\text{Ne}$ versus Fe/Mg data would fall along this dotted line, which is clearly not the case. On an event-by-event basis, the variations in $^{22}\text{Ne}/^{20}\text{Ne}$ are large, and, indeed, many of the high $^{22}\text{Ne}/^{20}\text{Ne}$ events have low Fe/Mg, which is in the wrong direction according to the Breneman & Stone (1985) interpretation.

As can be seen in Figures 6 and 7, $^{22}\text{Ne}/^{20}\text{Ne}$ and $^{26}\text{Mg}/^{24}\text{Mg}$ are clearly correlated with Fe/Mg when averaged over many events. From Figure 7, since we measure both the relative abundances and the charge states, we can test if a Breneman & Stone (1985) (power law in Q/A) relationship is applicable. The dashed line shows the prediction of this relationship for the magnesium and neon isotopes, based upon the measured charge states and the Fe/Mg abundances. Clearly, a power law in Q/A is not sufficient to explain the data. Similarly, Galvin et al. (2000), using elemental abundances measured by ACE/SEPICA, also found that a power law in Q/A did not produce a consistently good fit to their data. In fact, in our case, the discrepancy is so large that it is likely that the Q/A dependence is much more complicated than a simple monotonically changing function and may involve, for example, a resonance effect at certain Q/A values (e.g., Cohen et al. 2000). Of course, it is also possible that the abundance variations are not determined by Q/A alone and that other mechanisms are involved, e.g., a mass-dependent fractionation due to gravitational settling. However, at this time the inclusion of additional parameters in acceleration models is largely speculation.

Mewaldt et al. (1999), using 24–72 MeV nucleon⁻¹ ACE/SIS data, found that the ²²Ne/²⁰Ne enhancements were consistent with those of Na/Mg, which is more similar in both mass and Q/A than Fe/Mg. The events in their data set, however, were the most intense events seen by ACE. Of the SIS events that were also measured by ULEIS, most were in our ³He-“low” subset of events, which tended to have smaller ²²Ne/²⁰Ne fluctuations at 1 MeV nucleon⁻¹.

Because the difference in Q/A for ²²Ne and ²⁰Ne is only 10%, much smaller than the ~40% difference in Q/A for Mg and Fe, it is quite surprising that the variations in ²²Ne/²⁰Ne are so large when compared to the variations in Fe/Mg. That ³He is enhanced by enormous factors, while not understood in detail, can be explained by the fact that it uniquely has a $Q/A = \frac{2}{3}$, thus allowing resonant heating with turbulence in the plasma. That both the neon and magnesium isotopes are enhanced for ³He-“high” events shows that, like the heavy elements, a Q/A fractionation is likely occurring for the isotopes as well, although the magnitude is surprisingly large when compared to Fe/Mg.

Given that ²²Ne/²⁰Ne and ²⁶Mg/²⁴Mg correlate with ³He/⁴He and that the enhancements in all three of these isotope ratios are too large to be explained by a Breneman & Stone (1985) relation, we believe that the observations presented here are best explained by a mixing of two SEP components, i.e., by the mixing of the impulsive flare material, rich in ²²Ne, ²⁶Mg, ³He, and Fe (with high charge states), with the gradual, CME-associated material, which has at most modest enhancements in these species. In other words, all the variation in the abundance ratios as a function of ³He/⁴He, seen in the figures in this paper, arises simply from adding together, in varying degrees, a population with large abundance enhancements with a population with small abundance enhancements. This idea is consistent with the results of Mason, Mazur, & Dwyer (1999b), who measured significantly elevated amounts of ³He in large gradual SEP events. Because the time intensity profiles of the ³He, lasting several days, matched that of the major species, e.g., H, He, C, O, Fe, etc., Mason et al. (1999b) speculated that impulsive SEPs were part of a seed population that was further accelerated by the CME-driven shock.

As can be seen in Figures 2–6, the low abundance data (*left side of the plots*) and the high abundance data (*right side of the plots*) are smoothly joined together, indicating that the impulsive (³He-“high”) and the gradual (³He-“low”) SEP populations are somehow connected. It would be quite a coincidence if the mechanism that produces the abun-

dance enhancements in the gradual, CME-associated events results in abundances that connect up perfectly with those of the impulsive, flare-associated events.

The plateau in the Fe/O curve seen on the right side of Figures 3–5, and to some extent in the ²²Ne/²⁰Ne and Fe/Mg curves in Figure 6, is consistent with the earlier results of Mason et al. (1986) and Reames et al. (1994), who found no correlation with Fe enrichments and ³He/⁴He for ³He/⁴He > 0.1. It appears that for the impulsive events, the ³He/⁴He can change by orders of magnitude without a corresponding change in the other abundances. For instance, for one event in Figure 3, ³He/⁴He > 30, and yet the Fe/O was just barely over 1. This suggests that while the average values of ²²Ne, ²⁶Mg, and Fe are large in ³He-“high” events, the variation in these abundances may not depend strongly on the ³He/⁴He value. As a result, the presence of ³He may indicate that the source region and the acceleration mechanisms are different for some of the particles and not how strongly the enhancement mechanism is working at the acceleration site.

Finally, we note that while our data in Figure 7, which shows the abundances versus the average iron charge state, are consistent with the mixing of gradual and impulsive SEPs, other observations with SEPICA indicate that the linear relation between the abundances and the charge states that would be expected from mixing did not produce the best fit to the data (Möbius et al. 1999).

In summary, ACE/ULEIS has observed enhancements in ²²Ne/²⁰Ne, ²⁶Mg/²⁴Mg, and Fe/Mg that appear to be too large to be explained by a simple Q/A dependence (e.g., by a power law in Q/A). Furthermore, the enhancements are also associated with elevated ³He/⁴He values, indicating the presence of impulsive SEP material. How impulsive SEP events can produce such large elemental and isotopic enhancements is not clear at this point. However, the isotopic abundance measurements presented should provide new constraints on particle acceleration models, particularly models of energetic particle acceleration associated with flares.

We thank the many individuals at the University of Maryland and the Johns Hopkins Applied Physics Laboratory for the construction of the ULEIS instrument and at the University of New Hampshire and the Max-Planck-Institut für extraterrestrische Physik for their efforts on the SEPICA instrument. This work was supported in part by NASA grant PC 251428 and NAG 5-6912.

REFERENCES

- Anders, E., & Ebihara, M. 1982, *Geochim. Cosmochim. Acta*, 46, 2363
 Breneman, H. H., & Stone, E. C. 1985, *ApJ*, 299, L57
 Cohen, C. M. S., et al. 2000, in *AIP Conf. Proc. 528, Acceleration and Transport of Energetic Particles Observed in the Heliosphere*, ed. R. A. Mewaldt, J. R. Jokipii, M. A. Lee, E. Möbius, & T. H. Zurbuchen (New York: AIP), 55
 Fisk, L. A. 1978, *ApJ*, 224, 1048
 Galvin, A. B., et al. 2000, in *AIP Conf. Proc. 528, Acceleration and Transport of Energetic Particles Observed in the Heliosphere*, ed. R. A. Mewaldt, J. R. Jokipii, M. A. Lee, E. Möbius, & T. H. Zurbuchen (New York: AIP), 127
 Gosling, J. T. 1993, *J. Geophys. Res.*, 98, 18937
 Hsieh, K. C., & Simpson, J. A. 1970, *ApJ*, 162, L191
 Lee, M. A. 2000, in *AIP Conf. Proc. 528, Acceleration and Transport of Energetic Particles Observed in the Heliosphere*, ed. R. A. Mewaldt, J. R. Jokipii, M. A. Lee, E. Möbius, & T. H. Zurbuchen (New York: AIP), 3
 Leske, R. A., et al. 1999, in *Proc. 26th ICRC (Salt Lake City)*, SH 1.4.20, 6, 139
 Mason, G. M., Dwyer, J. R., & Mazur, J. E. 2000, *ApJ*, 545, L157
 Mason, G. M., et al. 1998, *Space Sci. Rev.*, 86, 409
 ———. 1999a, *Geophys. Res. Lett.*, 26, 141
 Mason, G. M., Mazur, J. E., & Dwyer, J. R. 1999b, *ApJ*, 525, L133
 Mason, G. M., Mazur, J. E., & Hamilton, D. C. 1994, *ApJ*, 425, 843
 Mason, G. M., Reames, D. V., Klecker, B., Hovestadt, D., & von Rosenvinge, T. T. 1986, *ApJ*, 303, 849
 Mazur, J. E., Mason, G. M., Looper, M. D., Leske, R. L., & Mewaldt, R. A. 1999, *Geophys. Res. Lett.*, 26, 173
 Mewaldt, R. A., et al. 1999, in *Proc. 26th ICRC (Salt Lake City)*, SH 1.4.17, 6, 127
 Meyer, J. P. 1985, *ApJS*, 57, 151
 Möbius, E., et al. 1998, *Space Sci. Rev.*, 86, 449
 ———. 1999, in *Proc. 26th ICRC (Salt Lake City)*, SH 1.4.07, 6, 87

- Möbius, E., et al. 2000, in AIP Conf. Proc. 528, Acceleration and Transport of Energetic Particles Observed in the Heliosphere, ed. R. A. Mewaldt, J. R. Jokipii, M. A. Lee, E. Möbius, & T. H. Zurbuchen (New York: AIP), 131
- Ogilvie, K. W., Coplan, M. A., Bochsler, P., & Geiss, J. 1980, J. Geophys. Res., 85, 6021
- Reames, D. V. 1999, Space Sci. Rev., 90, 413
- Reames, D. V., Meyer, J. P., & von Rosenvinge, T. T. 1994, ApJS, 90, 649
- Reames, D. V., von Rosenvinge, T. T., & Lin, R. P. 1985, ApJ, 292, 716
- Temerin, M., & Roth, I. 1992, ApJ, 391, L105
- von Steiger, R., et al. 2000, J. Geophys. Res., 105, 27217
- Wimmer-Schweingruber, R. F., et al. 1999, Geophys. Res. Lett., 26, 165